Correlating Aggregation Kinetics and Stationary Diffusion in Protein−Sodium Salt Systems Observed with Dynamic Light Scattering

Jonathan Rubin,[†,‡] Adriana San Miguel,[†] Andreas S. Bommarius,*[,†,‡,§] and Sven H. Behrens[†]

School of Chemical and Biomolecular Engineering and Parker H. Petit Institute of Bioengineering and Bioscience, Georgia Institute of Technology, 315 Ferst Drive, Atlanta, Georgia 30332-0363, and School of Chemistry and Biochemistry, Georgia Institute of Technology, 901 Atlantic Drive, Atlanta, Georgia 30332-0400

Received: December 23, 2009; Revised Manuscript Received: February 3, 2010

This paper compares two manifestations of electrolyte-mediated interaction between globular proteins. Salt-induced protein aggregation is studied with dynamic light scattering (DLS) in solutions of lysozyme and bovine serum albumin (BSA) containing different types of sodium salts. The same types of ions are used in a second measurement series assessing the effect of more dilute electrolytes on protein diffusivity in non-aggregating protein dispersions. Both aggregation and stable diffusion exhibit strong ion specificity along the lines of the Hofmeister series: chaotropic counterions act as the strongest coagulants and, in stable protein solutions, lead to the lowest "protein interaction parameter", evaluated as the slope of protein diffusivity versus protein concentration. Within this common qualitative trend, lysozyme and BSA solutions show marked differences, including the sign of the interaction parameter for most of the tested solution compositions. Despite the different nature of lysozyme and BSA, a strong correlation is found in both cases between the ion-specific interaction parameter and the proteins' aggregation tendency as indicated by the salt concentration required for fast aggregation. The interaction parameter, available via quick and easy DLS measurements on stable protein solutions, may thus serve as a predictor of ion-specific aggregation trends.

Introduction

Protein stability against aggregation is critically important for both disease markers and therapeutic agents. Protein aggregates are associated with neurodegenerative diseases such as Alzheimer's, Huntington's, and Parkinson's disease among many others.[1] In biotechnology, irreversible protein aggregation is a frequently prevalent problem in the production, formulation, shipping, and storage of therapeutic proteins. Many therapeutic proteins are on the market, and hundreds more are in clinical and preclinical trials.[2] Proteins that are currently on the market are prescribed to treat conditions such as diabetes, hemophilia, and myocardial infarction. Aggregation of these proteins is undesirable because it reduces protein efficacy[3] and violates FDA regulations requiring pharmaceutical proteins to be stable both physically and chemically for 18−24 months.[4]

Protein aggregation is strongly dependent on environmental factors such as temperature, pH, cosolutes, salt type, and concentration.[2] While protein unfolding, amyloid formation,[5] and even enzyme deactivation[6−9] have begun to be understood as a function of effects manifested through the Hofmeister series, the effects of salt type on protein aggregation are not understood, despite recent success at capturing and modeling their kinetics.[10,11] Often therapeutic proteins are solubilized, sterilized, and purified under harshly denaturing conditions (6 M GdnHCl, 8 M urea). Aggregation is easily initiated under such conditions and propagates through noncovalent interactions and interprotein disulfide bonding,[12] ultimately limiting biological yield. Understanding protein interaction at the onset of aggregation can help determine optimal processing and storage conditions so that aggregation losses can be minimized.[13]

While the analysis of later aggregation stages represents considerable challenges,[14] the rate constant k_{11} of doublet formation is more easily accessible. This rate constant is defined by[15,16]

$$\lim_{t\to 0} \frac{dN_1}{dt} = -k_{11}{N_0}^2 \tag{1}$$

where N_1 is the number concentration of singlets and N_0 the initial number concentration of monomers before coagulation takes place. Both thermodynamic and hydrodynamic interactions between the proteins influence the coagulation rate constant k_{11}. In the approximation of irreversible aggregation between isotropically interacting, spherical proteins, k_{11} can be calculated as[17]

$$k_{11} = \left[\int_{2a}^{\infty} \frac{\exp(u(r)/k_B T)}{4\pi r^2 D(r)}\, dr\right]^{-1} \tag{2}$$

Here, a is the protein radius, $k_B T$ the thermal energy unit, $u(r)$ the pair interaction energy, and $D(r)$ the separation dependent pair diffusion constant, which takes into account the hydrodynamic drag and rises monotonically[18] from zero at contact to the limiting value:

$$\lim_{r\to\infty} D(r) = 2D_0 \tag{3}$$

where D_0 is the familiar single particle diffusion constant described by the Stokes−Einstein relation:

* To whom correspondence should be addressed. E-mail: Andreas.Bommarius@chbe.gatech.edu.
† School of Chemical and Biomolecular Engineering.
‡ Parker H. Petit Institute of Bioengineering and Bioscience.
§ School of Chemistry and Biochemistry.

10.1021/jp912126w
Published on Web 02/23/2010

$$D_0 = \frac{k_B T}{6\pi\eta a} \tag{4}$$

(η is the solution viscosity). In the useful reference case of "sticky" but otherwise noninteracting spheres, eqs 2−4 lead to the well-known Smoluchowski rate constant $k_{11} = k_S$ with

$$k_S = \frac{8k_B T}{3\eta} \tag{5}$$

From eq 2, it is clear that repulsive particle interactions and hydrodynamic drag both contribute to stabilize dispersions against aggregation, but the complex interaction between real proteins in solution is not captured nearly well enough by the existing models to permit quantitative predictions. Experimentally, k_{11} can be obtained with relative ease using dynamic light scattering (DLS). The initial increase of the protein's hydrodynamic radius at the onset of aggregation satisfies eq 6:[19]

$$\frac{1}{r_h(0)}\left(\frac{dr_h(t)}{dt}\right)_{t\to 0} = \frac{I_2(q)}{2I_1(q)}\left(1 - \frac{r_{h,1}}{r_{h,2}}\right)k_{11}N_1 \tag{6}$$

where r_h is defined in analogy to eq 4 as $r_h(t) = k_B T/6\pi\eta D_0(t)$, $r_h(0)$ is the initial value before aggregation sets in, $r_{h,1}$ and $r_{h,2}$ are the hydrodynamic radii of a single protein and a doublet, respectively, and I_1 and I_2 are their scattering intensities. The scattering intensities in principle depend on the scattering angle through the wave vector **q**. However, the small proteins considered in this study act as point scatterers for the 633 nm laser wavelength used ($qr_h \ll 1$); therefore, we may safely approximate $I_2/2I_1$ as unity. Using the geometric relation $r_{h,2}/r_{h,1} = 1.38$ for spheres,[19] and the measured initial change in size, we can solve for the coagulation rate constant k_{11}.

Interestingly, the mark of protein−protein interactions can be found not only in the time dependence of protein diffusivity in dilute aggregating systems but also in the concentration dependence of protein diffusivity in nonaggregating systems. In stable protein solutions, protein−protein interaction leads to a concentration dependence of the mutual diffusion coefficient:

$$D(c) = D_0[1 + \nu c + O(c^2)] \tag{7}$$

This diffusion coefficient and, by extension, the coefficient ν in the virial expansion 7 are readily accessible to dynamic light scattering.[20] The coefficient ν, known as the interaction parameter,[13] sums up first-order effects of both thermodynamic and hydrodynamic particle−particle interactions in dispersions, with hydrodynamic coupling and repulsive thermodynamic interactions both leading to an increase in $D(c)$ for the case of spherical particles.[21,22] For protein systems, the precise interplay of thermodynamic and hydrodynamic contributions cannot currently be predicted, and attempts to disentangle these two contributions experimentally are fraught with difficulty.[13] In this study, we take a pragmatic, semiempirical approach to correlate the net interaction parameter ν of stable protein solutions with aggregation kinetics in unstable solutions of similar ion composition but higher ionic strength, retaining in either case both thermodynamic and hydrodynamic contributions.

Two model proteins, lysozyme and bovine serum albumin (BSA), were chosen to investigate the relative stabilization or destabilization of protein dispersions that arise in different electrolyte solutions due to Hofmeister effects[24] (for a review on the state of Hofmeister effects, see Kunz[23]). Lysozyme and BSA were chosen because they have been studied extensively and have been established as models for protein−solution and protein−protein interactions. Both proteins are readily available at high purity and assume a roughly spherical conformation in stable solutions.[13,25]

The present study examines ion specificity of salt-induced protein aggregation. Using DLS, diffusion coefficients and aggregation rate constants for both proteins are established. The two physical parameters are then related, and we find a strong correlation between protein diffusivity in nonaggregating systems (mutual diffusion coefficients) and aggregating systems (aggregation rate constants). This paper presents a convenient way of inferring information about medium-specific aggregation tendencies from stable protein samples.

Materials and Methods

Protein Purification and Preparation. Deionized water was used to prepare all solutions. Lysozyme was obtained from Sigma-Aldrich (St. Louis, MO; >90% purity) and was dissolved in an aqueous sodium acetate (Sigma-Aldrich, >99% purity) and acetic acid (Riedel-de-Haen, 96% purity) buffer of pH 4.25. The solution was then filtered using a Whatman Anotop 10, 0.02 μm pore size filter. Filtration removed larger proteins and any other relevant contaminants detectable by electrophoresis or DLS. The true concentration of protein was then calculated using a Beckman Coulter DU 800 spectrophotometer at 280 nm and using an extinction coefficient of 26.3/mmol/cm.[26]

Bovine serum albumin, Fraction V, was obtained from EMD (Gibbstown, NJ, >98% purity) and dissolved in an acetate buffer. The dissolved BSA was then filtered using a Pall Acrodisc syringe filter, 0.2 μm Supor Membrane. The filtered solution was subsequently loaded onto a GE Healthcare HiPrep 16/60 Sephacryl High Resolution size exclusion chromatography column using an Amersham Pharmacia Biotech AKTAexplorer FPLC. The proper elution fractions were collected and concentrated using a 30 kDa MW cutoff Pall JumboSep centrifugal membrane filter. The concentrated solution was then filtered with a Whatman Anotop 10, 0.02 μm pore size filter, and tested for purity using SDS-PAGE gel electrophoresis.

Electrolyte Buffer Preparation. All salts used were of >99% purity, ACS reagent grade. Salt solutions were made in acetate solutions as described above containing one of the following: sodium sulfate anhydrous (Sigma-Aldrich), sodium formate (Aldrich), sodium phosphate monobasic (Sigma-Aldrich), sodium fluoride (BDH), sodium chloride (BDH), sodium bromide (Sigma-Aldrich), sodium nitrate (Sigma-Aldrich), or sodium iodide (EMD). The pH was then adjusted using either sodium hydroxide or the appropriate acid (i.e., sulphuric acid for a sulfate solution). The salt solution was filtered using a Pall Acrodisc syringe filter, 0.2 μm Supor Membrane.

Mutual Diffusion Coefficient Experiments. Diffusivity measurements were carried out at 25 °C, pH 4.25,[27] and total ionic strength 0.1 M, 50 mM acetate and 50 mM of the salt in question. These conditions ensured that the protein was in a globular conformation, since the melting point of both proteins in similar solutions is significantly higher (~75 °C for lysozyme[28] and ~60 °C for BSA[29]).

Salt solutions were mixed with protein solutions of varying protein concentration in a low volume Sarstedt UV-transparent disposable cuvette. The sample was stirred very gently to avoid shear-induced aggregation and to homogenize the solution. The protein−salt solution was then inserted into a Malvern Zetasizer

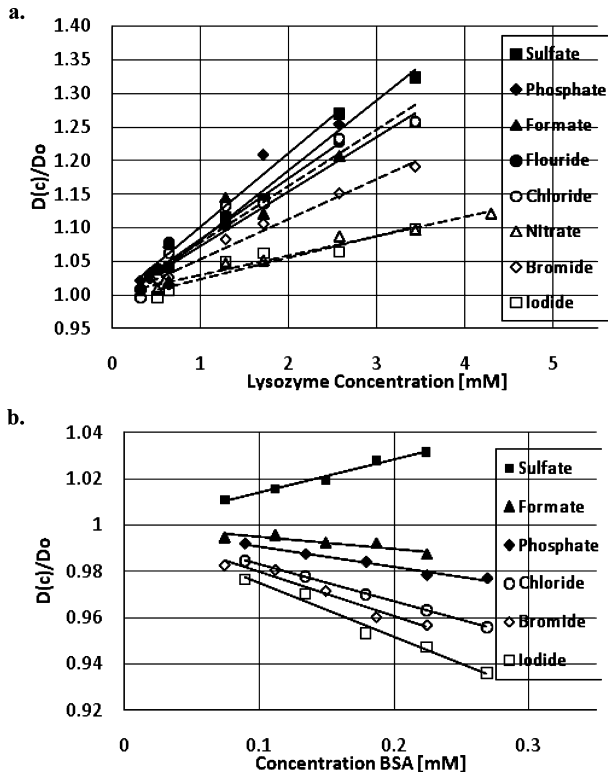

Figure 1. Plots of normalized relative mutual diffusion coefficient as a function of protein concentration. Experiments were run at pH 4.25, $T = 25$ °C, and $I = 0.1$ M arising to 50% from acetate buffer and 50% from the indicated sodium salt, with the exception of sodium sulfate, which was diluted by a factor of 2^6 compared to the monovalent ions, as explained in the text. (a) The top plot is for lysozyme, $D_0 = (7.57 \pm 0.4) \times 10^{-11}$ m^2/s; (b) the lower plot is for BSA, $D_0 = (3.27 \pm 0.1) \times 10^{-11}$ m^2/s.

Nano ZS for measurement. Twelve runs of 30 s each were taken and averaged.

Aggregation Rate Experiments. All aggregation rate experiments were performed at 25 °C and with a 100 mM acetate background buffer. Lysozyme experiments were performed at pH 4.25.[27] BSA experiments were run at pH 4. The lower pH for BSA was chosen to distance the aggregation experiments from BSA's isoelectric point, 4.7.[30]

Samples were prepared similarly to the mutual diffusion coefficient experiments; however, in these experiments, a wide range of salt molarities were investigated. Protein−salt solutions were prepared in cuvettes, and then *quickly* inserted into the Zetasizer. The change in particle hydrodynamic radius was monitored for at least 60 min.

Results and Discussion

Interaction Parameters. Parts a and b of Figure 1 show the relative diffusivity of lysozyme and BSA, respectively, in stable sodium salt solutions of increasing protein concentrations. The slope of each curve represents the interaction parameter ν specific for the given ion and ionic strength. Larger ν values are indicative of stronger stabilizing (repulsive) protein−protein interaction. The inferred ν values for chaotropic counterions (dashed lines, open icons) vary substantially and generally correlate with the Hofmeister series, with ν decreasing with increasingly chaotropic counterions (Table 1). For kosmotropes (solid lines, filled icons), ν values are larger by comparison and for lysozyme they are uniform, whereas, for BSA, they are not but do generally correlate with the Hofmeister series as

TABLE 1: Ionic Strength I_s of Solution at k_s ($k_{11} = 10^{-17}$ m^3/s), the Interaction Parameter ν, and Experimental Jones−Dole B Viscosity Coefficients[33]

	Lysozyme		BSA		
ion	I_s (M)	ν (1/M)	I_s (M)	ν (1/M)	Jones−Dole B[33]
I^-	0.23	32 ± 5	0.15	-232 ± 19	−0.068
NO_3^-	0.28	29 ± 2			−0.046
Br^-	0.55	60 ± 4	0.36	-193 ± 24	−0.032
Cl^-	1.51	84 ± 8	0.67	-161 ± 2	−0.007
HCO_2^-		81 ± 9	1.01	-50 ± 14	0.052
$H_2PO_4^-$	1.55	111 ± 9	0.8	-89 ± 8	0.340
F^-		89 ± 6			0.1
SO_4^{2-}	1.63	105 ± 8	1.41	143 ± 11	0.208

evidenced by the progression of increasing ν values as we go from chaotropic to kosmotropic counterions. Sulfate is a notable outlier if used at the same molarity as the other ions (not shown). If used at a molarity lower by a factor of 2^6, however, the results for sulfate fit squarely into the small range observed for the other kosmotropes for lysozyme, as shown (this relation was also used for BSA). A scaling with the inverse sixth power of the counterion valency is familiar from the classical Schulze−Hardy rule for the critical coagulation concentration (CCC) of charged colloidal particles.[31] We shall see below that the connection with coagulation kinetics goes even further.

The values of ν for lysozyme are positive, whereas most of the values for BSA are negative, implying that BSA is more prone to aggregation than lysozyme in general (confirmed by comparing Figure 3a and b). Despite the difference in sign, the same Hofmeister trend is apparent in both cases and it is important to note that propensity to aggregate is dictated by *relative* differences in ν for a given protein. In both cases, sulfate had a large positive ν, suggesting that it will strongly stabilize either protein at the given conditions. This is likely due to sulfate being by far the most kosmotropic counterion used, which would be expected to stabilize strongly.

Kosmotropes are thought to promote water structure, whereas chaotropes are expected to "break water structure" and interact preferentially with the protein.[21] As a result, chaotropes will tend to accumulate *at* the protein surface while kosmotropes will be concentrated in the water bulk *away from* the protein. The observed variations between different chaotropes may thus be caused by ion−protein interaction of varying strength. By the same token, the relative similarity of the kosmotropes for lysozyme may stem from their common tendency of being depleted from a zone, the *excluded volume*, around the protein.

For a given counterion, the protein−protein interaction depends on the ionic strength of the solution, and so does the absolute value of ν. At ionic strengths sufficiently high to induce protein aggregation, ν becomes inaccessible to DLS because the single protein diffusivity is masked by an ever changing distribution of aggregates. It seems plausible, however, that, of several stable protein solutions with different salt types but similar (valency-adjusted) concentration, the ones with the strongest stabilizing interaction should require the largest increase in ionic strength in order to induce aggregation. We therefore hypothesize that the *relative* values of the measured ν are a robust (and quick!) predictor for the counterion-specific protein aggregation tendency.

Aggregating Protein Concentration Independence. Before beginning aggregation experiments, we confirmed that the coagulation rate constant k_{11} was independent of the initial concentration of either protein, N_1, for both chaotropes and kosmotropes. While this independence would clearly be ex-

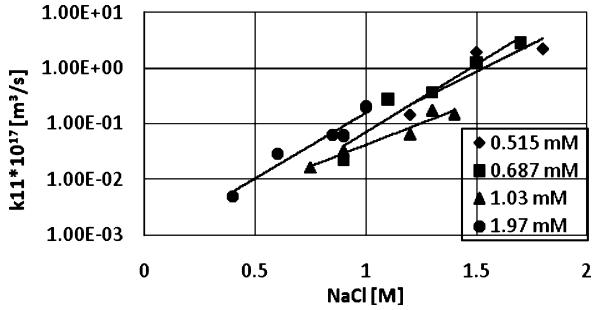

Figure 2. Coagulation rate constants for lysozyme−NaCl systems using different lysozyme concentrations. Icons represent different lysozyme molarities. Within experimental uncertainty, the four protein molarities yield essentially the same rate constant for a given salt molarity.

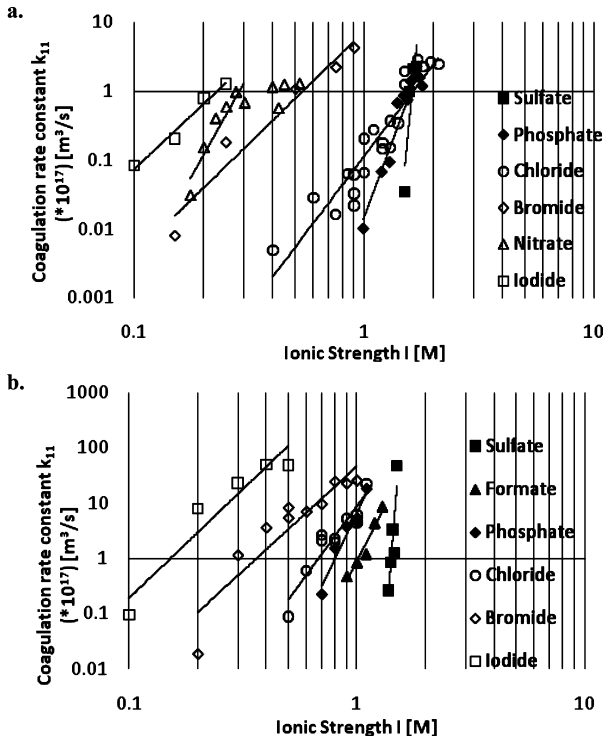

Figure 3. Coagulation rate constant, k_{11}, as a function of ionic strength. (a) Lysozyme experiments were run at pH 4.25 and $T = 25$ °C in a 0.1 M sodium acetate buffer (top). (b) BSA experiments were run at pH 4.0 and $T = 25$ °C in a 0.1 M sodium acetate buffer (bottom).

pected for colloidal particles, it is not obvious for proteins which can undergo rapid conformational changes upon partial unfolding or denaturing.[32] Figure 2 shows that k_{11} for lysozyme−chloride systems is the same despite changing the lysozyme concentration, confirming that our rate constant is in fact a rate *constant*.

Protein Aggregation Kinetics. Like the diffusivities (Figures 1), our results for the aggregation rate constant k_{11} (Figure 3) again show marked differences between the chaotropes, whereas the kosmotropes display relatively uniform behavior for lysozyme and a general Hofmeister trend for BSA. The results follow a clear Hofmeister trend for both proteins, with the most chaotropic ions inducing aggregation at the lowest ion strength. The ionic strength required for kosmotropes to induce fast aggregation was very similar for lysozyme, ~1.5 M. At lower ionic strength, in the slow aggregation regime, even these more kosmotropic solutions for lysozyme show a Hofmeister trend for both proteins as BSA does.

Table 1 summarizes the important findings from the two sets of experiments. The theoretical Smoluchowski rate constant of

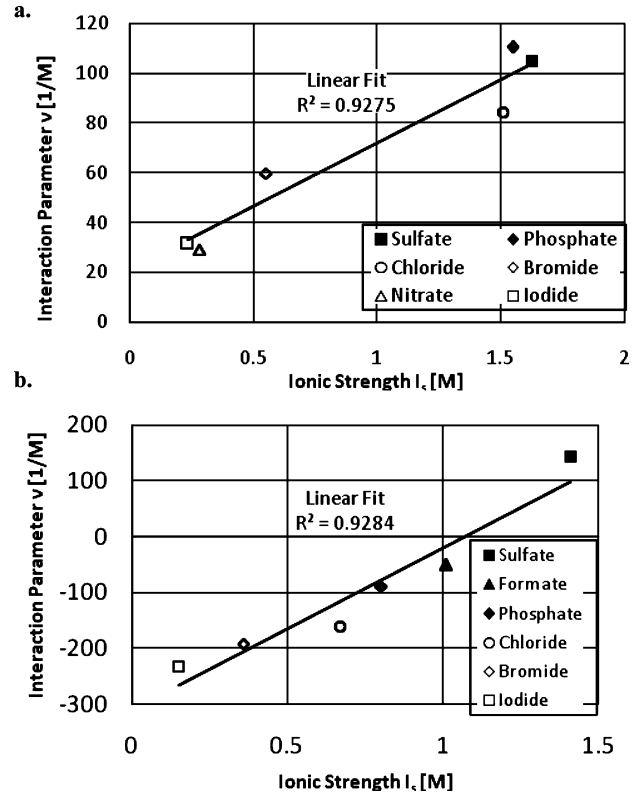

Figure 4. Relating ν and ionic strength at $k_{11} = 10^{-17}$ m^3/s. (a) Correlation for lysozyme; (b) correlation for BSA.

fast aggregation, eq 5, is on the order of 10^{-17} m^3/s for the studied systems (it assumes exactly that value for 2.4 M chloride solution). The value of $k_{11} = 10^{-17}$ m^3/s was therefore chosen as a reference and the ionic strength I_s required to reach this reference condition was tabulated (Table 1) as a measure for the ion-specific resistance toward aggregation.

Correlating ν and I_s. Figure 4 shows a strong correlation between ν and I_s, which is quantified by a linear correlation coefficient of $R^2 = 0.93$ for both lysozyme and BSA. The Hofmeister trend is expressed in the fact that both ν and I_s increase gradually from the highly chaotropic (iodide) to very kosmotropic (sulfate) solutions.

These plots confirm our hypothesis that protein aggregation can be predicted using the interaction parameter of stable solutions at low ionic strength. This correlation is very useful because characterizing aggregation kinetics, as in Figure 3, can take days or even weeks, as opposed to finding the interaction parameter which can be done in less than 30 min.

The two proteins studied have different functions and size (lysozyme MW= 14.4 kDa; BSA MW= 67 kDa), and markedly different values for ν, with sulfate solutions representing an outlier only in the case of BSA, but not for lysozyme (Figure 1). Despite all of these inherent differences, there is, for both proteins, a strong correlation between the ion-specific interaction parameter ν and the ionic strength I_s required to induce fast aggregation with the given type of ion. This insensitivity of the correlation seen in Figure 4 to differences in protein properties instills confidence in the robustness of predictions for aggregation tendencies from DLS data on stable solutions.

Conclusion

In this work, we studied the mutual diffusion coefficients and coagulation rate constants for lysozyme and BSA in sodium salt systems using dynamic light scattering. For both proteins

and both experiments, we found stabilizing trends against aggregation akin to the Hofmeister series. Chaotrope-induced aggregation at lower ionic strengths had lower interaction parameters ν, that exhibited variance between each other, whereas kosmotropes required much higher ionic strengths to aggregate, and had larger ν values. This work suggests that ν for stable protein systems can be used for *quick* and easy predictions of ion-specific aggregation trends. The observations for sulfate in the BSA system are unparalleled in the lysozyme system, and we do not have a satisfying explanation at this point. Nonetheless, the correlation works beautifully for two very different proteins and is thus shown to be remarkably robust!

Acknowledgment. Funding for this project was provided by GAANN and the GA Tech Integrative BioSystems Initiative (IBSI). We thank Dr. Adrian Katona for his pioneering efforts with lysozyme and Dr. William Koros' lab for use of their refractometer. J.R. would like to dedicate this paper to Drs. Viviane Yargeau and David G. Cooper of McGill University for inspiring his research career.

Supporting Information Available: Refractive index measurements, trendline linearization equations, illustrative calculation of k_{11}, and selected CCC values found. This material is available free of charge via the Internet at http://pubs.acs.org.

References and Notes

(1) Lansbury, P. T. *Biophys. J.* **1999**, *76*, A258.
(2) Chi, E. Y.; Krishnan, S.; Randolph, T. W.; Carpenter, J. F. *Pharm. Res.* **2003**, *20*, 1325.
(3) Mitraki, A.; King, J. *Bio/Technology* **1989**, *7*, 690.
(4) Cleland, J. L.; Powell, M. F.; Shire, S. J. *Crit. Rev. Ther. Drug Carrier Syst.* **1993**, *10*, 307.
(5) Yeh, V.; Broering, J. M.; Chen, B.; Romanyuk, A.; Chernoff, Y. O.; Bommarius, A. S. *Protein Sci.* **2010**, *19*, 47–56.
(6) Bommarius, A. S.; Karau, A. *Biotechnol. Prog.* **2005**, *21*, 1663.
(7) Broering, J. M.; Bommarius, A. S. *J. Phys. Chem. B* **2005**, *109*, 20612.
(8) Broering, J. M.; Bommarius, A. S. *Biochem. Soc. Trans.* **2007**, *35*, 1602.
(9) Broering, J. M.; Bommarius, A. S. *J. Phys. Chem. B* **2008**, *112*, 12768.
(10) Andrews, J. M.; Roberts, C. J. *Biochemistry* **2007**, *46*, 7558.
(11) Roberts, C. J. *Biotechnol. Bioeng.* **2007**, *98*, 927.
(12) Militello, V.; Casarino, C.; Emanuele, A.; Giostra, A.; Pullara, F.; Leone, M. *Biophys. Chem.* **2004**, *107*, 175.
(13) Liu, W.; Cellmer, T.; Keerl, D.; Prausnitz, J. M.; Blanch, H. W. *Biotechnol. Bioeng.* **2005**, *90*, 482.
(14) Lattuada, M.; Wu, H.; Sandkuhler, P.; Sefcik, J.; Morbidelli, M. *Chem. Eng. Sci.* **2004**, *59*, 1783.
(15) Barany, S.; Cohen Stuart, M. A.; Fleer, G. J. *Colloids Surf.* **1996**, *106*, 213.
(16) Holthoff, H.; Egelhaaf, S. U.; Borkovec, M.; Schurtenberger, P.; Sticher, H. *Langmuir* **1996**, *12*, 5541.
(17) Behrens, S. H.; Borkovec, M. *J. Colloid Interface Sci.* **2000**, *225*, 460.
(18) Honig, E. P.; Roebersen, G. J.; Wiersema, P. H. *J. Colloid Interface Sci.* **1971**, *36*, 97.
(19) Holthoff, H.; Schmitt, A.; Fernandez Barbero, A.; Borkovec, M.; CabrerizoVilchez, M. A.; Schurtenberger, P.; HidalgoAlvarez, R. *J. Colloid Interface Sci.* **1997**, *192*, 463.
(20) Berne, B. J. P. R. *Dynamic Light Scattering*; Wiley: New York, 1979.
(21) Dickinson, E. *Annu. Rep. Prog. Chem., Sect. C* **1983**, *80*, 3.
(22) Russel, W. B.; Saville, D. A.; Schowalter, W. R. *Colloidal Dispersions*; Cambridge University Press: Cambridge, U.K., 1989.
(23) Kunz, W.; Lo Nostro, P.; Ninham, B. W. *Curr. Opin. Colloid Interface Sci.* **2004**, *9*, 1.
(24) Zhang, Y.; Cremer, P. S. *Curr. Opin. Chem. Biol.* **2006**, *10*, 658.
(25) Tu, R. S.; Breedveld, V. *Phys. Rev. E* **2005**, *72*, 041914.
(26) Steiner, R. F. *Biochim. Biophys. Acta* **1964**, *79*, 51.
(27) Georgalis, Y.; Umbach, P.; Raptis, J.; Saenger, W. *Acta Crystallogr., Sect. D* **1997**, *53*, 691.
(28) Jacob, J.; Krafft, C.; Welfle, K.; Welfle, H.; Saenger, W. *Acta Crystallogr., Sect. D* **1998**, *54*, 74.
(29) Arakawa, T.; Kita, Y. *Biochim. Biophys. Acta* **2000**, *1479*, 32.
(30) Ku, J. R.; Stroeve, P. *Langmuir* **2004**, *20*, 2030.
(31) Hiemenz, P. C.; Rajagopalan, R. *Principles of colloid and surface chemistry*, 3rd ed.; Marcel Dekker: New York, 1997.
(32) Smith, L. J.; Fiebig, K. M.; Schwalbe, H.; Dobson, C. M. *Fold Des.* **1996**, *1*, R95.
(33) Collins, K. D. *Biophys. J.* **1997**, *72*, 6.

JP912126W